One-atom maser: Phase-sensitive measurements

Berthold-Georg Englert, Tserensodnom Gantsog,* Axel Schenzle,† Christian Wagner,‡ and Herbert Walther‡
Max-Planck-Institut für Quantenoptik, Hans-Kopfermann-Strasse 1, D-85748 Garching, Germany
(Received 10 July 1995)

We reconsider a variant of the one-atom-maser setup in which the emerging atoms are probed for coherent superpositions of the two Rydberg states of the maser transition. The statistical properties of the corresponding detector clicks contain information about the temporal evolution of the phase of the quantized electromagnetic field inside the resonator. We derive analytical expressions for certain statistical quantities, such as the mean number of successive clicks of the same kind, or the atom-atom and the photon-photon correlation functions. The latter are closely related if the photon-number distribution in steady state is dominated by a single narrow peak.

PACS number(s): 84.40.Ik, 03.65.−w, 32.80.−t, 42.50.Dv

I. INTRODUCTION

In standard one-atom-maser (OAM) experiments [1], the atoms enter the resonator in the upper one of the two Rydberg states of the maser transition and the emerging atoms are probed for being in either one of these two states. The statistical properties of the emerging atoms, or rather of the corresponding detector clicks, are determined experimentally and then compared with the theoretical predictions. In this way, a certain regime of the OAM dynamics has been investigated thoroughly, viz., the regime that is relevant for the photon-number distribution in steady state and closely related properties of the quantized electromagnetic field inside the resonator. The agreement between the results of OAM experiments and the predictions of OAM theory [2] has been very satisfactory as yet.

If one wishes, however, to test other aspects of the OAM dynamics, such as those that determine the shape of the maser line, the setup has to be modified so that the experimental data become sensitive to the phase properties of the cavity field. Two possibilities are suggested: one imposes a phase either through the preparation of the entering atoms or through the detection of the emerging atoms — the choice is between a preselection or a postselection of the phase. The first possibility is to pump the resonator with a controlled phase by preparing the arriving atoms in a coherent superposition of the masing states. This setup is suffering from the obvious drawback that the dynamics is changed and, among other things, the steady state is altered. This is clearly undesirable. The second, better, possibility [3–5] avoids such modifications of the dynamics inasmuch as the final detection of the atoms is done differently, not their initial preparation. In this scheme, the detectors respond to coherent superpositions of the atomic states rather than to the states themselves as in the standard OAM experiments. The quantum-mechanical reduction of the photon state that is associated with the registration of a detector click imposes a phase on the photon state, a phase that depends on which one of the detectors has clicked. Predictions about the next atom to come are sensitive to this phase and so the phase dynamics can be tested experimentally.

In the present paper we reconsider the setup of Refs. [3–5] in which the phase of the quantized cavity field is postselected. We are interested in the statistical properties of the detector clicks, since the click statistics constitutes the reproducible experimental data. In particular, we derive an analytical expression for the mean number of successive clicks of the same kind. This quantity has been computed in Refs. [3–5] with the aid of a Monte Carlo method. We find perfect agreement between those numerical results and the analytical answer. The analytical expression tells us which aspects of the OAM dynamics enter this mean number, a highly valuable insight that is not supplied by the Monte Carlo computation. It turns out that, contrary to what was surmised in Refs. [3–5], the said mean number does not contain the sought information about the phase dynamics. Therefore, we also study the correlations between emerging atoms (or rather between detector clicks) where this information is available. The unobservable photon-photon correlation function, whose Fourier transform supplies us with the maser spectrum, is related to the atom-atom correlation function, which can be determined experimentally. We discuss the conditions under which this relation is close.

Finally, we present a brief outlook on conceivable future developments aimed at demonstrating that the atom-atom correlations violate the Bell inequality [6]. The three-atom correlations that are built up by the OAM interaction can also be studied by the techniques used in this paper. In particular, one could systematically look for strong correlations of the Greenberger-Horne-Zeilinger type [7].

II. SETTING THE STAGE

The setup of the standard OAM experiments is schematically recalled in Fig. 1(a). The atom arrives in the upper state $|A\rangle$ of the maser transition, traverses the cavity, and is then probed for its final state. If the atom is found to be still in state $|A\rangle$, then no photon has been emitted in effect during the interaction of the two-level atom with the photons in the resonator; if the atom is detected in the lower state $|B\rangle$, how-

*Permanent address: Department of Theoretical Physics, National University of Mongolia, 210646 Ulaanbaatar, Mongolia.
†Also at Sektion Physik, Universität München, Theresienstrasse 37/III, D-80333 München, Germany.
‡Also at Sektion Physik, Universität München, Am Coulombwall 1, D-85748 Garching, Germany.

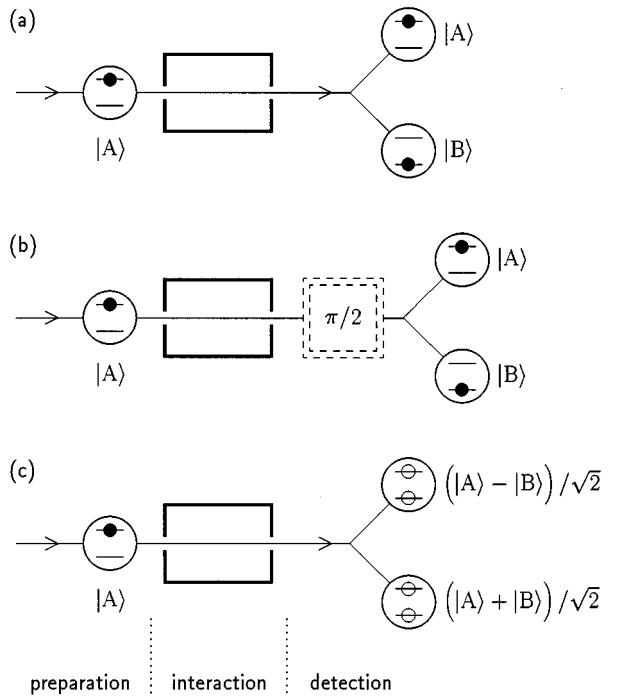

FIG. 1. Schematic setups of one-atom-maser experiments. In the standard setup (a), atoms are prepared in the upper state $|A\rangle$, interact with the photons in the resonator, and are then detected in $|A\rangle$ or in the lower state $|B\rangle$. In the phase-sensitive setup (b), the atoms experience a $\pi/2$ pulse before reaching the detectors. This setup is equivalent to (c), where the $\pi/2$ pulse is regarded as part of the detection device so that, in effect, the emerging atoms are probed for being in the superpositions $(|A\rangle \mp |B\rangle)/\sqrt{2}$.

ever, then one photon has been added to the cavity field.

In the setup proposed in Refs. [3–5], which is depicted in Fig. 1(b), the atom crosses a classical microwave field after exiting from the cavity and before reaching the detectors that discriminate between states $|A\rangle$ and $|B\rangle$. This microwave field is resonant with the $|A\rangle \leftrightarrow |B\rangle$ transition. Its strength is such that it effects a $\pi/2$ pulse and so turns $|A\rangle$ into the coherent superposition $(|A\rangle + |B\rangle)/\sqrt{2}$ and $|B\rangle$ into $(|B\rangle - |A\rangle)/\sqrt{2}$ [8]. Inasmuch as the detectors probe for $|A\rangle$ and $|B\rangle$, a more appropriate way of looking at the effect of the $\pi/2$ pulse states that $(|A\rangle - |B\rangle)/\sqrt{2}$ is turned into $|A\rangle$ and $(|A\rangle + |B\rangle)/\sqrt{2}$ into $|B\rangle$. The latter point of view regards the classical microwave field as part of the detection device. This leads us to the picture of Fig. 1(c), where the emerging atoms are probed for being in one of the two coherent superpositions $(|A\rangle \mp |B\rangle)/\sqrt{2}$. Of course, Fig. 1(c) refers to quite the same experimental apparatus as does Fig. 1(b).

The statistical operator ρ describes the photon state inside the resonator. It is a function of the ladder operators $a^\dagger$ and a that create and annihilate quanta of the privileged mode of the quantized electromagnetic field. The two-level atom interacts resonantly with the photons in this mode. Prior to the interaction, the combined state of the atom-photon system is

$$\mathrm{P}_{\mathrm{before}} = |A\rangle\rho\langle A| = \rho\sigma^\dagger\sigma, \tag{2.1}$$

with the atomic ladder operators

$$\sigma = |B\rangle\langle A|, \quad \sigma^\dagger = |A\rangle\langle B|. \tag{2.2}$$

According to well-known results of OAM theory [9–11], the net effect of the interaction is summarized in the transition

$$\mathrm{P}_{\mathrm{before}} \rightarrow \mathrm{P}_{\mathrm{after}} = S_A\rho S_A^\dagger\sigma^\dagger\sigma + S_B\rho S_B^\dagger\sigma\sigma^\dagger + S_A\rho S_B^\dagger\sigma^\dagger + S_B\rho S_A^\dagger\sigma, \tag{2.3}$$

where the sandwich operators

$$S_A = \cos(\varphi\sqrt{aa^\dagger}),$$
$$S_B = a^\dagger\frac{\sin(\varphi\sqrt{aa^\dagger})}{\sqrt{aa^\dagger}} \tag{2.4}$$

involve the accumulated Rabi angle φ.

In the standard OAM setup of Fig. 1(a) the observation of a click of the detector for $|A\rangle$ states implies a final photon state that is obtained by the state reduction

$$\mathrm{P}_{\mathrm{after}} \rightarrow \mathcal{A}\rho/\ \mathrm{tr}\{\mathcal{A}\rho\}, \tag{2.5}$$

where we establish contact with the notational conventions of Ref. [12] clicks. The linear operator $\mathcal{A}$ is herein given by

$$\mathcal{A}\rho \equiv S_A\rho S_A^\dagger. \tag{2.6}$$

Likewise, a click of the $|B\rangle$ detector is accompanied by

$$\mathrm{P}_{\mathrm{after}} \rightarrow \mathcal{B}\rho/\ \mathrm{tr}\{\mathcal{B}\rho\} \tag{2.7}$$

with

$$\mathcal{B}\rho \equiv S_B\rho S_B^\dagger. \tag{2.8}$$

If the atoms are not observed, or the detector clicks are deliberately ignored [13], the change in ρ resulting from the passage of one atom is

$$S_A\rho S_A^\dagger + S_B\rho S_B^\dagger - \rho = (\mathcal{A} + \mathcal{B} - 1)\rho. \tag{2.9}$$

Since the atoms arrive randomly in an uncorrelated fashion at a beam rate of r, the photon state evolves according to the master equation

$$\frac{\partial}{\partial t}\rho = [\mathcal{L} + r(\mathcal{A} + \mathcal{B} - 1)]\rho \equiv \mathcal{L}^{(0)}\rho. \tag{2.10}$$

The symbol $\mathcal{L}$ denotes the familiar Liouville operator that models the decay of the cavity field to the thermal state

$$\rho^{(\mathrm{th})} = \frac{1}{\nu + 1}\left(\frac{\nu}{\nu + 1}\right)^{a^\dagger a}. \tag{2.11}$$

with ν thermal photons. In explicit terms, $\mathcal{L}$ reads

$$\mathcal{L}\rho = -\frac{\Gamma}{2}(\nu + 1)(a^\dagger a\rho - 2a\rho a^\dagger + \rho a^\dagger a) - \frac{\Gamma}{2}\nu(aa^\dagger\rho - 2a^\dagger\rho a + \rho aa^\dagger), \tag{2.12}$$

whereby the photon lifetime equals $1/\Gamma$.

An analogous analysis can be performed for the phase sensitive setup of Fig. 1(b). When treating it in the spirit of Fig. 1(c), one recognizes immediately that the operators $\mathcal{A}$ and $\mathcal{B}$ of (2.6) and (2.8) are replaced by

$$\left.\begin{matrix}\mathcal{A}\rho\\ \mathcal{B}\rho\end{matrix}\right\}=\frac{1}{2}(S_{\mathrm{A}}\rho S_{\mathrm{A}}^{\dagger}+S_{\mathrm{B}}\rho S_{\mathrm{B}}^{\dagger})\mp\frac{1}{2}(S_{\mathrm{A}}\rho S_{\mathrm{B}}^{\dagger}+S_{\mathrm{B}}\rho S_{\mathrm{A}}^{\dagger}). \tag{2.13}$$

For these, Eq. (2.9) is equally valid, and so is the master equation (2.10), of course.

Therefore the steady state $\rho^{(\mathrm{SS})}$ of the OAM, which obeys $\mathcal{L}^{(0)}\rho^{(\mathrm{SS})}=0$, is the same for both setups, the standard one of Fig. 1(a) and the phase sensitive one of Figs. 1(b) and 1(c). It has the well-known form [9]

$$\rho^{(\mathrm{SS})}(a^{\dagger}a)=\rho^{(\mathrm{SS})}(0)\prod_{n=1}^{a^{\dagger}a}\left[\frac{\nu}{\nu+1}+\frac{r/\Gamma}{\nu+1}\,\frac{\sin^2(\varphi\sqrt{n})}{n}\right], \tag{2.14}$$

with $\rho^{(\mathrm{SS})}(0)$ determined by the normalization of $\rho^{(\mathrm{SS})}$ to unit trace. Since $\rho^{(\mathrm{SS})}$ is a function of the photon number $a^{\dagger}a$, not of $a^{\dagger}$ and a individually, the Fock-state matrix of $\rho^{(\mathrm{SS})}$ is diagonal. This property is conserved by the state reductions (2.5) and (2.7) if $\mathcal{A}$ and $\mathcal{B}$ are the operators (2.6) and (2.8) of the standard OAM setup. In sharp contrast, the state reductions produced by $\mathcal{A}$ and $\mathcal{B}$ of (2.13) couple neighboring diagonals. In particular, they turn a diagonal state $\rho(a^{\dagger}a)$ into a tridiagonal one. In this situation, the expectation value $\langle a\rangle=\mathrm{tr}\{a\rho\}$ of the photon ladder operator a is nonzero after the state reduction, although it vanished before. Upon recalling that the numerical phase of the complex number $\langle a\rangle$ is the phase of the electromagnetic field associated with the photon state, one recognizes that this property of the operators (2.13) makes the scheme of Refs. [3–5] phase sensitive.

Another important difference between the two schemes concerns the evolution of the photon state ρ between successive detector clicks, that is, between state reductions. This is not just the free decay generated by $\mathcal{L}$ of (2.12) because one has to account for the changes produced by those atoms that escape detection. According to Ref. [12], this evolution between clicks is governed by the nonlinear master equation

$$\frac{\partial}{\partial t}\rho=\{\mathcal{L}+[1-\tfrac{1}{2}(\eta_{\mathrm{A}}+\eta_{\mathrm{B}})]r(\mathcal{A}+\mathcal{B}-1)\}\rho$$
$$-\tfrac{1}{2}(\eta_{\mathrm{A}}-\eta_{\mathrm{B}})r[\mathcal{A}-\mathcal{B}-\mathrm{tr}\{(\mathcal{A}-\mathcal{B})\rho\}]\rho, \tag{2.15}$$

where $\eta_{\mathrm{A}},\eta_{\mathrm{B}}$ are the detector efficiencies. If the emerging atoms are not observed, $\eta_{\mathrm{A}}=\eta_{\mathrm{B}}=0$, then this equation is equal to (2.10), as it should be.

For the two $\mathcal{A},\mathcal{B}$ pairs — one of (2.6) and (2.8), the other of (2.13) — the sum $\mathcal{A}+\mathcal{B}$ is the same, but the difference $\mathcal{A}-\mathcal{B}$ is not. As a consequence, the first, linear, contribution on the right-hand side of (2.15) does not discriminate between the two schemes, but the second, nonlinear, one does. Whereas it is true that this second contribution is absent if the detection is symmetric, $\eta_{\mathrm{A}}=\eta_{\mathrm{B}}$, the distinction between the two schemes is essential nevertheless, because one of the detector efficiencies may be effectively zero in a specific calculation. For example, this is the case when one is considering correlations among the detector clicks of one kind only.

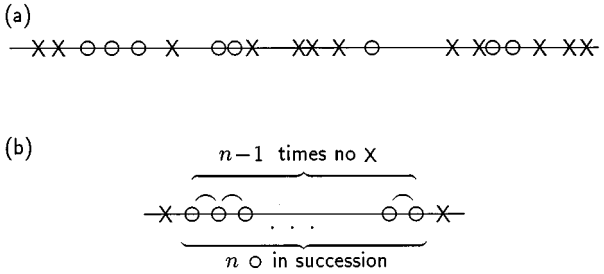

FIG. 2. (a) A sequence of events of two kinds, symbolized by circles ○ and crosses X, consists of strings of successive events of just one kind. (b) For each string of n successive ○ events there are $n-1$ strings with no X event and vice versa.

For future reference, we note that Eq. (2.15) is solved by

$$\rho(t)=\frac{\exp(\mathcal{L}^{(\eta)}t)\rho(0)}{\mathrm{tr}\{\exp\,(\mathcal{L}^{(\eta)}t)\rho(0)\}}, \tag{2.16}$$

where

$$\mathcal{L}^{(\eta)}\equiv\mathcal{L}^{(0)}-r(\,\eta_{\mathrm{A}}\mathcal{A}+\,\eta_{\mathrm{B}}\mathcal{B}) \tag{2.17}$$

is a linear operator, albeit one for which $\exp(\mathcal{L}^{(\eta)}t)$ is not trace conserving (unless $\eta_{\mathrm{A}}=\eta_{\mathrm{B}}=0$, of course). One verifies that (2.16) obeys (2.15) by differentiation in conjunction with the identity

$$\mathrm{tr}\{(\mathcal{A}+\mathcal{B})\rho\}=\mathrm{tr}\{\rho\}, \tag{2.18}$$

which is a fundamental property of the operators $\mathcal{A}$ and $\mathcal{B}$.

The stage is now set. We turn to the calculation of the mean number of detector clicks of the same kind first and then to atom-atom and photon-photon correlation functions. To the extent to which the general results do not depend on the particular form of $\mathcal{A}$ and $\mathcal{B}$, we shall be dealing with both OAM setups on an equal footing — indeed with all OAM setups.

III. SUCCESSIVE CLICKS OF THE SAME KIND

A. General considerations

Consider an arbitrary sequence of events of two kinds, such as the clicks of the $|\mathrm{A}\rangle$ and $|\mathrm{B}\rangle$ detectors or the crosses and circles that are used in Fig. 2 for illustration. The physical nature of the events is utterly irrelevant in this subsection. It does not matter at all whether we are dealing with random events or with ones that are strongly correlated.

We denote the probability (or relative frequency) for having exactly n events of one kind between two successive events of the other kind by p_n with $n=0,1,2,3,\ldots$. For each count of n events of one kind there are $n-1$ counts of zero events of the other kind; see Fig. 2(b). Therefore the sum rule

$$p_0=\sum_{n=1}^{\infty}(n-1)p_n \tag{3.1}$$

holds. We combine it with the normalization

$$\sum_{n=0}^{\infty}p_n=1 \tag{3.2}$$

to arrive at the statement

$$\sum_{n=1}^{\infty}np_n=1\,. \tag{3.3}$$

Let us now ask a slightly different question. How large are the probabilities P_n for getting n events of the same kind in succession? The way of counting is different here because n cannot equal zero for conceptual reasons. The probabilities P_n are thus normalized in accordance with

$$\sum_{n=1}^{\infty}P_n=1\,. \tag{3.4}$$

Except for discarding the $n=0$ possibility, there is no essential difference between the probabilities p_n and P_n, so that

$$P_n=\frac{p_n}{\sum_{m=1}^{\infty}p_m}=\frac{p_n}{1-p_0} \tag{3.5}$$

relates them to each other; the latter equality is implied by the normalization (3.2).

The quantity we are interested in is $\overline{n}$, the average number of successive events of the same kind [14],

$$\overline{n}\equiv\sum_{n=1}^{\infty}nP_n\,. \tag{3.6}$$

As an immediate consequence of (3.5) and (3.3) this number is given by

$$\overline{n}=\frac{1}{1-p_0}, \tag{3.7}$$

so that we simply need to calculate p_0, which is the probability that there are no events of one kind between two successive events of the other kind.

B. Uncorrelated events

Before considering the correlated OAM clicks it is instructive to calculate p_0 for uncorrelated events. The corresponding value of $\overline{n}$, for which we write $\overline{n}_{\rm uncor}$, will serve as a useful benchmark for judging the OAM values of $\overline{n}$.

We treat the case of ''two successive A events with no B events in between'' in detail; the reverse case is handled by exchanging the labels A and B consistently. These are the ingredients: the rates at which the uncorrelated events occur are $r_{\rm A}$ and $r_{\rm B}$; the probability that the first event is of type A equals $r_{\rm A}/(r_{\rm A}+r_{\rm B})$; the probability to have another A event after the elapse of $t\cdots t+dt$ is $r_{\rm A}$dt; the probability that there was no other A event in the meantime is $\exp(-r_{\rm A}t)$; the probability that there was no B event is $\exp(-r_{\rm B}t)$. The multiplication of these probabilities and the integration over the temporal spacing t of the two successive A events produces

$$\int_0^{\infty}dt\;r_{\rm A}\frac{r_{\rm A}}{r_{\rm A}+r_{\rm B}}e^{-r_{\rm A}t}e^{-r_{\rm B}t}=\left(\frac{r_{\rm A}}{r_{\rm A}+r_{\rm B}}\right)^2. \tag{3.8}$$

After adding the analogous contribution for two successive B events, obtained by the interchange $r_{\rm A}\leftrightarrow r_B$, we get

$$p_0=\frac{r_{\rm A}^2+r_{\rm B}^2}{(r_{\rm A}+r_{\rm B})^2}=1-\frac{2r_{\rm A}r_{\rm B}}{(r_{\rm A}+r_{\rm B})^2}. \tag{3.9}$$

The mean number of successive uncorrelated events is therefore given by

$$\overline{n}_{\rm uncor}=\frac{(r_{\rm A}+r_{\rm B})^2}{2r_{\rm A}r_{\rm B}}\geqslant 2\,. \tag{3.10}$$

The lower bound of two recognizes that $\overline{n}_{\rm uncor}$ is twice the squared ratio of the arithmetic and geometric means of $r_{\rm A}$ and $r_{\rm B}$. Therefore, the equal sign applies only for $r_{\rm A}=r_{\rm B}$.

If $\overline{n}=\overline{n}_{\rm uncor}$ is found for a given sequence of events, one cannot, of course, conclude that there are no correlations among the events. Any deviation of $\overline{n}$ from $\overline{n}_{\rm uncor}$, however, indicates the presence of correlations. Roughly speaking, the events are bunched if $\overline{n}>\overline{n}_{\rm uncor}$ and antibunched if $\overline{n}<\overline{n}_{\rm uncor}$. In particular, the extreme value of $\overline{n}=1$ characterizes a strictly alternating sequence of A and B events — perfect antibunching in other words.

C. Correlated OAM clicks

1. General results

Mutatis mutandis, the calculation of $\overline{n}$ for OAM clicks follows the general pattern that produced $\overline{n}_{\rm uncor}$ in Sec. III.B. Owing to the correlations among the clicks, the details are more involved. We shall make extensive use of the methods and results of Ref. [12]. Alternatively and equivalently, one could argue in the spirit of Ref. [15], or possibly [16], and arrive at the same answers.

The *a priori* rates for the clicks of the $|{\rm A}\rangle$ and $|{\rm B}\rangle$ detectors are

$$r_{\rm A}=r\,\eta_{\rm A}\,{\rm tr}\{\mathscr{A}\rho^{(\rm SS)}\},\quad r_{\rm B}=r\,\eta_{\rm B}\,{\rm tr}\{\mathscr{B}\rho^{(\rm SS)}\}, \tag{3.11}$$

with the symbols introduced in Sec. II. As in Sec. III B, the probability that the first click is of type A is given by the relative rate $r_{\rm A}/(r_{\rm A}+r_{\rm B})$. After this first A click the photon state is

$$\rho_{\rm A}(0)=\frac{\mathcal{A}\rho^{(\rm SS)}}{{\rm tr}\{\mathcal{A}\rho^{(\rm SS)}\}}; \tag{3.12}$$

this is the state reduction (2.5) applied to the steady state $\rho^{(\rm SS)}$ of (2.14). Until the next click happens, this state evolves according to the master equation (2.15). After the elapse of time t we thus have [cf. Eq. (2.16)]

$$\rho_{\rm A}(t)=\frac{\exp(\mathcal{L}^{(\eta)}t)\rho_{\rm A}(0)}{{\rm tr}\{\exp\,(\mathcal{L}^{(\eta)}t)\rho_{\rm A}(0)\}}. \tag{3.13}$$

The probability for having an A click at time $t\cdots t+dt$ is therefore given by

$$r\ dt\,\eta_{\mathrm{A}}\,\mathrm{tr}\{\mathcal{A}\rho_{\mathrm{A}}(t)\} \tag{3.14}$$

and the probability that there was no A click in the meantime is the exponentiated time integral thereof,

$$\exp\left(-r\int_0^t dt'\,\eta_{\mathrm{A}}\,\mathrm{tr}\,\{\mathcal{A}\rho_{\mathrm{A}}(t')\}\right). \tag{3.15}$$

Since the analogous probability for no B click is obtained by the replacement $\eta_{\mathrm{A}}\mathcal{A}\rightarrow\eta_{\mathrm{B}}\mathcal{B}$, the probability for no click of either kind in the meantime is

$$\exp\left(-r\int_0^t dt'\ \mathrm{tr}\,\{(\eta_{\mathrm{A}}\mathcal{A}+\eta_{\mathrm{B}}\mathcal{B})\rho_{\mathrm{A}}(t')\}\right). \tag{3.16}$$

Putting things together, we have the preliminary result [compare with (3.8)]

$$\begin{aligned}p_0=&\int_0^\infty dt\,\frac{r_{\mathrm{A}}}{r_{\mathrm{A}}+r_{\mathrm{B}}}r\,\eta_{\mathrm{A}}\,\mathrm{tr}\{\mathcal{A}\rho_{\mathrm{A}}(t)\}\\&\times\exp\left(-r\int_0^t dt'\ \mathrm{tr}\,\{(\eta_{\mathrm{A}}\mathcal{A}+\eta_{\mathrm{B}}\mathcal{B})\rho_{\mathrm{A}}(t')\}\right)\\&+[\mathrm{A}\leftrightarrow\mathrm{B}],\end{aligned} \tag{3.17}$$

where the symbolic last term represents the contribution of two successive B clicks.

Considerable simplifications can be achieved. First note that the identity

$$-r\ \mathrm{tr}\{\ (\eta_{\mathrm{A}}\mathcal{A}+\eta_{\mathrm{B}}\mathcal{B})\rho\}=\ \mathrm{tr}\{\mathcal{L}^{(\eta)}\rho\}, \tag{3.18}$$

valid for any ρ, implies that the no-click probability (3.16) is equal to the denominator in (3.13),

$$\begin{aligned}&\exp\left(-r\int_0^t dt'\ \mathrm{tr}\,\{(\eta_{\mathrm{A}}\mathcal{A}+\eta_{\mathrm{B}}\mathcal{B})\rho_{\mathrm{A}}(t')\}\right)\\&=\exp\left(\int_0^t dt'\,\frac{\mathrm{tr}\,\{\mathcal{L}^{(\eta)}\exp(\mathcal{L}^{(\eta)}t')\rho_{\mathrm{A}}(0)\}}{\mathrm{tr}\,\{\exp\,(\mathcal{L}^{(\eta)}t')\rho_{\mathrm{A}}(0)\}}\right)\\&=\exp\left(\int_0^t dt'\,\frac{\partial}{\partial t'}\ln\mathrm{tr}\,\{\exp\,(\mathcal{L}^{(\eta)}t')\rho_{\mathrm{A}}(0)\}\right)\\&=\mathrm{tr}\,\{\exp\,(\mathcal{L}^{(\eta)}t)\rho_{\mathrm{A}}(0)\}.\end{aligned} \tag{3.19}$$

Then we use (3.11)–(3.13) to establish

$$\begin{aligned}&r_{\mathrm{A}}\,\mathrm{tr}\{\mathcal{A}\rho_{\mathrm{A}}(t)\}\,\mathrm{tr}\,\{\exp\,(\mathcal{L}^{(\eta)}t)\rho_{\mathrm{A}}(0)\}\\&=r\,\eta_{\mathrm{A}}\,\mathrm{tr}\,\{\mathcal{A}\,\exp(\mathcal{L}^{(\eta)}t)\mathcal{A}\rho^{(\mathrm{SS})}\}.\end{aligned} \tag{3.20}$$

Consequently, an equivalent expression for p_0 is [17]

$$\begin{aligned}p_0=&\int_0^\infty dt\,\frac{r^2}{r_{\mathrm{A}}+r_{\mathrm{B}}}[\,\eta_{\mathrm{A}}\,\mathrm{tr}\,\{\mathcal{A}\,\exp(\mathcal{L}^{(\eta)}t)\mathcal{A}\rho^{(\mathrm{SS})}\}\\&+\eta_{\mathrm{B}}^2\,\mathrm{tr}\,\{\mathcal{B}\,\exp(\mathcal{L}^{(\eta)}t)\mathcal{B}\rho^{(\mathrm{SS})}\}]\\=&\frac{r^2}{r_{\mathrm{A}}+r_{\mathrm{B}}}[\,\eta_{\mathrm{A}}^2\,\mathrm{tr}\,\{\mathcal{A}[-\mathcal{L}^{(\eta)}]^{-1}\mathcal{A}\rho^{(\mathrm{SS})}\}\\&+\eta_{\mathrm{B}}^2\,\mathrm{tr}\,\{\mathcal{B}[-\mathcal{L}^{(\eta)}]^{-1}\mathcal{B}\rho^{(\mathrm{SS})}\}].\end{aligned} \tag{3.21}$$

Next, we observe that the equality $(\mathcal{L}^{(0)}-\mathcal{L}^{(\eta)})/r-\eta_{\mathrm{B}}\mathcal{B}=\eta_{\mathrm{A}}\mathcal{A}$ in conjunction with $\mathcal{L}^{(0)}\rho^{(\mathrm{SS})}=0$ and, for any ρ, $\mathrm{tr}\{\mathcal{L}^{(0)}\rho\}=0$ supplies the two statements

$$\begin{aligned}&\eta_{\mathrm{A}}^2\,\mathrm{tr}\,\{\mathcal{A}[-\mathcal{L}^{(\eta)}]^{-1}\mathcal{A}\rho^{(\mathrm{SS})}\}\\&=r_{\mathrm{A}}/r^2-\eta_{\mathrm{A}}\eta_{\mathrm{B}}\,\mathrm{tr}\,\{\mathcal{B}[-\mathcal{L}^{(\eta)}]^{-1}\mathcal{A}\rho^{(\mathrm{SS})}\}\end{aligned} \tag{3.22a}$$

$$=r_{\mathrm{A}}/r^2-\eta_{\mathrm{A}}\eta_{\mathrm{B}}\,\mathrm{tr}\,\{\mathcal{A}[-\mathcal{L}^{(\eta)}]^{-1}\mathcal{B}\rho^{(\mathrm{SS})}\}, \tag{3.22b}$$

where the definition of r_{A} in (3.11) has entered. We combine that statement about $\eta_{\mathrm{B}}^2\,\mathrm{tr}\,\{\mathcal{B}[-\mathcal{L}^{(\eta)}]^{-1}\mathcal{B}\rho^{(\mathrm{SS})}\}$ that corresponds to (3.22a) with (3.22b) and turn (3.21) into

$$p_0=1-\frac{2r^2}{r_{\mathrm{A}}+r_{\mathrm{B}}}\,\eta_{\mathrm{A}}\eta_{\mathrm{B}}\,\mathrm{tr}\,\{\mathcal{A}[-\mathcal{L}^{(\eta)}]^{-1}\mathcal{B}\rho^{(\mathrm{SS})}\}. \tag{3.23}$$

According to (3.7), the mean number of successive OAM detector clicks of the same kind is therefore given by

$$\overline{n}=\frac{r_{\mathrm{A}}+r_{\mathrm{B}}}{2r^2}(\,\eta_{\mathrm{A}}\eta_{\mathrm{B}}\,\mathrm{tr}\,\{\mathcal{A}[-\mathcal{L}^{(\eta)}]^{-1}\mathcal{B}\rho^{(\mathrm{SS})}\}^{-1}, \tag{3.24}$$

which is a central result of this paper. In view of the symmetry expressed in (3.22) it is clear that the operators $\mathcal{A}$ and $\mathcal{B}$ could change their places in the trace without affecting the value of $\overline{n}$.

In the situation of very low detector efficiencies, that is, $0<\eta_{\mathrm{A}},\eta_{\mathrm{B}}\ll 1$, most of the atoms escape detection and the clicks are so infrequent that their correlations become irrelevant. Therefore consistency requires that $\overline{n}$ of (3.24) reduces to $\overline{n}_{\mathrm{uncor}}$ of (3.10) in this event. In the Appendix, we demonstrate that (3.24) passes this test indeed.

The no-click probability of (3.19) has to vanish in the limit of $t\rightarrow\infty$. As a consequence, all the eigenvalues $-\lambda_\mu^{(\eta)}$ of the linear operator $\mathcal{L}^{(\eta)}$ must have negative real parts. We denote the right eigenstates by $\rho_\mu^{(\eta)}$ and the left ones by $\check{\rho}_\mu^{(\eta)}$,

$$\mathcal{L}^{(\eta)}\rho_\mu^{(\eta)}=-\lambda_\mu^{(\eta)}\rho_\mu^{(\eta)},\quad \check{\rho}_\mu^{(\eta)}\mathcal{L}^{(\eta)}=-\lambda_\mu^{(\eta)}\check{\rho}_\mu^{(\eta)}. \tag{3.25}$$

[The left action $\check{\rho}\mathcal{M}$ of any Liouville operator $\mathcal{M}$ is related to its right action $\mathcal{M}\rho$ through the requirement that $\mathrm{tr}\{\check{\rho}\,(\mathcal{M}\rho)\}=\mathrm{tr}\{(\check{\rho}\,\mathcal{M})\rho\}$ holds for any pair $\check{\rho}$, ρ.] We normalize $\check{\rho}_\mu^{(\eta)}$ and $\rho_\mu^{(\eta)}$ such that the duality relation

$$\mathrm{tr}\{\check{\rho}_{\mu}^{(\eta)}\rho_{\mu'}^{(\eta)}\}=\delta_{\mu\mu'} \tag{3.26}$$

involves no numerical constants. Then the completeness statement

$$\rho=\sum_{\mu}\rho_{\mu}^{(\eta)}\,\mathrm{tr}\{\check{\rho}_{\mu}^{(\eta)}\rho\}, \tag{3.27}$$

which says that any ρ can be written as a weighted sum of the right eigenstates $\rho_{\mu}^{(\eta)}$, does not involve such constants either. With the eigenvalues and eigenstates of $\mathcal{L}^{(\eta)}$ at hand, spectral decompositions

$$f(\mathcal{L}^{(\eta)})\rho=\sum_{\mu}\rho_{\mu}^{(\eta)}f(-\lambda_{\mu}^{(\eta)})\,\mathrm{tr}\{\check{\rho}_{\mu}^{(\eta)}\rho\} \tag{3.28}$$

are available for functions of $\mathcal{L}^{(\eta)}$, in particular for the inverse $[-\mathcal{L}^{(\eta)}]^{-1}$. This offers a convenient way of evaluating the trace in (3.24), viz.,

$$\overline{n}=\frac{r_{\mathrm{A}}+r_{\mathrm{B}}}{2r}\left(\eta_{\mathrm{A}}\eta_{\mathrm{B}}\sum_{\mu}\mathrm{tr}\{\mathcal{A}\rho_{\mu}^{(\eta)}\}\frac{r}{\lambda_{\mu}^{(\eta)}}\mathrm{tr}\{\check{\rho}_{\mu}^{(\eta)}\mathcal{B}\rho^{(\mathrm{SS})}\}\right)^{-1}. \tag{3.29}$$

All the numerical results reported below have been produced in this manner. As a rule, the solution of the eigenvalue problem (3.25) is the most time-consuming part of a computation along these lines.

2. Perfect detectors

An exception is encountered in the situation of perfect detectors, that is, $\eta_{\mathrm{A}}=\eta_{\mathrm{B}}=1$. Actually, since there are no perfect detectors, one is here no longer considering the statistics of detector clicks but rather the statistics of the emerging atoms themselves. In this $\eta_{\mathrm{A}}=\eta_{\mathrm{B}}=1$ case, $\mathcal{L}^{(\eta)}$ of (2.17) differs from the Liouville operator $\mathcal{L}$ of the photon damping [specified in (2.12)] only by an additive constant,

$$\mathcal{L}^{(1)}\equiv\mathcal{L}^{(\eta)}|_{\eta_{\mathrm{A}}=\eta_{\mathrm{B}}=1}=\mathcal{L}-r. \tag{3.30}$$

The eigenvalues of $\mathcal{L}$ are

$$-\lambda_{k,n}=-(|k|/2+n)\Gamma, \tag{3.31}$$

with $k=0,\pm1,\pm2,\ldots$ and $n=0,1,2,\ldots$, and the eigenvalues of $-\mathcal{L}^{(1)}$ are given by $r+\lambda_{k,n}$. The pair k,n represents here the formal index μ in Eqs. (3.25)–(3.29). The corresponding common eigenstates $\rho_{k,n}$ and $\check{\rho}_{k,n}$ of $\mathcal{L}$ and $\mathcal{L}^{(1)}$ are the familiar members of the standard damping basis [18]. In particular, for $k=0$, $n=0$ we have the thermal state of (2.11) and the identity operator,

$$\rho_{0,0}=\rho^{(\mathrm{th})},\quad \check{\rho}_{0,0}=1\,. \tag{3.32}$$

Rather than repeating once more the explicit forms of $\rho_{k,n}$ and $\check{\rho}_{k,n}$, which involve normally ordered Laguerre polynomials, let us mention a convenient pair of generating functions [19], viz.,

$$\mathrm{P}(\alpha^*,\alpha)\equiv e^{-(\nu+1)\alpha^*\alpha}e^{\alpha a^\dagger}\rho^{(\mathrm{th})}e^{\alpha^* a}=\sum_{k,n}\alpha^{*n+(|k|-k)/2}\alpha^{n+(|k|+k)/2}\frac{(\nu+1)^{n+|k|}}{(n+|k|)!}\rho_{k,n} \tag{3.33}$$

and

$$\check{\mathrm{P}}(\alpha^*,\alpha)\equiv e^{-\nu\alpha^*\alpha}e^{\alpha a^\dagger}e^{\alpha^* a}=e^{-(\nu+1)\alpha^*\alpha}e^{\alpha^* a}e^{\alpha a^\dagger}=\sum_{k,n}\alpha^{*n+(|k|+k)/2}\alpha^{n+(|k|-k)/2}\frac{(\nu+1)^n}{n!}\check{\rho}_{k,n}\,. \tag{3.34}$$

The duality relation (3.26), here with $\delta_{\mu\mu'}=\delta_{kk'}\delta_{nn'}$, is equivalent to the statement

$$\mathrm{tr}\{\check{\mathrm{P}}(\alpha^*,\alpha)\mathrm{P}(\beta^*,\beta)\}=e^{(\nu+1)(\alpha^*\beta+\beta^*\alpha)}, \tag{3.35}$$

which is easily checked.

A few other important properties of $\rho_{k,n}$ and $\check{\rho}_{k,n}$ are worth recalling. Changing the sign of k is equivalent to taking the adjoint,

$$\rho_{-k,n}=(\rho_{k,n})^\dagger,\quad \check{\rho}_{-k,n}=(\check{\rho}_{k,n})^\dagger, \tag{3.36}$$

and therefore we can restrict the discussion to $k\geqslant0$. For these k values, the generating functions (3.33) and (3.34) tell us that $\rho_{k,n}$ is a certain function of the photon number $a^\dagger a$ multiplied by k factors of $a^\dagger$,

$$\rho_{k,n}(a^\dagger,a)=\left(a^\dagger\frac{1}{\sqrt{aa^\dagger}}\right)^k f_{k,n}(a^\dagger a)\quad\text{for}\quad k\geqslant0\,, \tag{3.37}$$

whereas $\check{\rho}_{k,n}$ is of the complementary form

$$\check{\rho}_{k,n}(a^\dagger,a)=\check{f}_{k,n}(a^\dagger a)\left(\frac{1}{\sqrt{aa^\dagger}}a\right)^k\quad\text{for}\quad k\geqslant0\,. \tag{3.38}$$

[The powers of $(aa^\dagger)^{-1/2}$, which turn $a^\dagger$ and a into normalized ladder operators, are introduced for later convenience; they simplify (3.50), for instance.] In other words, in the number state matrices of all $\rho_{n,k}$'s and all $\check{\rho}_{n,k}$'s only one side diagonal has nonzero entries (the kth below or above the main diagonal, respectively, for $k\geqslant0$). Thus the index k labels the diagonals and the index n labels the various eigenstates to a given diagonal. Roughly speaking, for larger n values the relevant photon numbers are larger too.

For $\eta_{\mathrm{A}}=\eta_{\mathrm{B}}=1$, Eqs. (3.11) and (2.18) imply the equality $r_{\mathrm{A}}+r_{\mathrm{B}}=r$, which states the obvious: if all atoms are detected, then the total click rate $r_{\mathrm{A}}+r_{\mathrm{B}}$ must equal the beam rate r. In summary, we find

$$\overline{n}=\left(\sum_{k,n}\mathrm{tr}\{\mathcal{A}\rho_{k,n}\}\frac{2r}{r+(|k|/2+n)\Gamma}\mathrm{tr}\{\check{\rho}_{k,n}\mathcal{B}\rho^{(\mathrm{SS})}\}\right)^{-1} \tag{3.39}$$

for the mean number of successive atoms in the same final state. Since all quantities on the right-hand side are known explicitly, the evaluation of this expression is quite straightforward.

3. Symmetric detectors

If the detector efficiencies are finite and equal, that is, $0<\eta_A=\eta_B<1$, then some of the attractive symmetry properties of the damping basis are also possessed by the eigenstates of $\mathcal{L}^{(\eta)}$. The numerical calculations are then technically much simpler than in the asymmetric situation $\eta_A \neq \eta_B$. Mainly for such practical reasons, all results reported below in Secs. IIIC4 and IIIC5 have been computed for symmetric detectors.

For $\eta_A=\eta_B\equiv\eta$, we can write $\mathcal{L}^{(\eta)}$ in the form

$$\mathcal{L}^{(\eta)}=[\mathcal{L}+(1-\eta)r(\mathcal{A}+\mathcal{B}-1)]-\eta r\equiv\tilde{\mathcal{L}}^{(0)}-\eta r, \tag{3.40}$$

where $\tilde{\mathcal{L}}^{(0)}$ is a Liouville operator of the OAM kind defined in (2.10) with a reduced beam rate of $\tilde{r}=(1-\eta)r$. Since $\tilde{\mathcal{L}}^{(0)}$, and therefore also $\mathcal{L}^{(\eta)}$, does not couple the diagonals of ρ to each other, their common eigenstates are of the single-diagonal type as well,

$$\rho_{k,n}^{(\eta)}(a^\dagger,a)=\left(a^\dagger\frac{1}{\sqrt{aa^\dagger}}\right)^k f_{k,n}^{(\eta)}(a^\dagger a),$$

$$\check{\rho}_{k,n}^{(\eta)}(a^\dagger,a)=\check{f}_{k,n}^{(\eta)}(a^\dagger a)\left(\frac{1}{\sqrt{aa^\dagger}}a\right)^k, \tag{3.41}$$

here, as in (3.37) and (3.38), stated for $k\geqslant 0$; since $\mathcal{L}^{(\eta)}$ is Hermitian in the sense of

$$[\mathcal{L}^{(\eta)}\rho]^\dagger=\mathcal{L}^{(\eta)}\rho^\dagger, \tag{3.42}$$

its eigenvalues $-\lambda_{k,n}^{(\eta)}$ make up pairs of complex numbers,

$$\lambda_{-k,n}^{(\eta)}=[\lambda_{k,n}^{(\eta)}]^*. \tag{3.43}$$

It is then both possible and natural to normalize the eigenstates $\rho_{k,n}^{(\eta)}$ and $\check{\rho}_{k,n}^{(\eta)}$ such that they obey (3.36). In particular, for $k=0$ the eigenvalues $-\lambda_{0,n}^{(\eta)}$ are real — and, in fact, negative — and the eigenstates $\rho_{0,n}^{(\eta)}$ and $\check{\rho}_{0,n}^{(\eta)}$ are Hermitian. For $k=0$, $n=0$ the statement analogous to (3.32) reads

$$\rho_{0,0}^{(\eta)}=\tilde{\rho}^{(\mathrm{SS})},\quad \check{\rho}_{0,0}^{(\eta)}=1,\quad \lambda_{0,0}^{(\eta)}=\eta r, \tag{3.44}$$

where $\tilde{\rho}^{(\mathrm{SS})}$ is the OAM steady state (2.14) with r replaced by the reduced rate $\tilde{r}=(1-\eta)r$.

The main difference between the $\eta<1$ case of this section and the $\eta=1$ case of Sec. III C 2 consists in our knowledge about the eigenvalues and eigenstates of $\mathcal{L}^{(\eta)}$. Whereas those for $\eta=1$ are well known explicitly, those for $\eta<1$ are presently only available numerically. Most other differences are minor and many are elementary. For instance, here Eqs. (3.11) and (2.18) imply $r_A+r_B=\eta r$, which is an obvious statement too. Then, the analog of (3.39) is

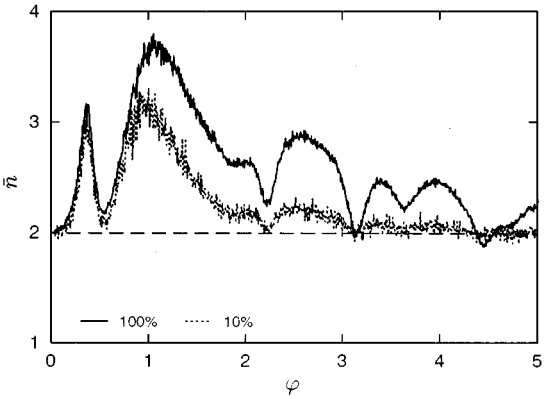

FIG. 3. Mean number $\overline{n}$ of successive detector clicks of the same kind in the phase-sensitive setup of Fig. 1(b) or 1(c). For $r/\Gamma=25/3$ and $\nu=0$, the values of $\overline{n}$ are shown for Rabi angles in the range $0<\varphi<5$ and for detector efficiencies of $\eta=100\%$ and 10%. The plot is the result of a Monte Carlo simulation; it is essentially identical to Fig. 3(a) of Ref. [5].

$$\overline{n}=\left(\sum_{k,n}\ \mathrm{tr}\,\{\mathcal{A}\rho_{k,n}^{(\eta)}\}\frac{2\eta r}{\lambda_{k,n}^{(\eta)}}\,\mathrm{tr}\,\{\check{\rho}_{k,n}^{(\eta)}\mathcal{B}\rho^{(\mathrm{SS})}\}\right)^{-1}. \tag{3.45}$$

Depending on the particular form of the operators $\mathcal{A}$ and $\mathcal{B}$, this can be simplified further, as we shall discuss in the subsequent sections.

4. Phase-sensitive setup

For the phase sensitive setup of Fig. 1(b) or 1(c), $\overline{n}$ has been computed recently in Refs. [3–5] by means of a Monte Carlo simulation that produced estimates for the probabilities P_n of Sec. IIIA. The Rabi angle φ covered the range $0<\varphi<5$ in these calculations while the ratio of the rates $r/\Gamma=25/3$ and the thermal photon number $\nu=0$ were kept at fixed values. Some of these results are reproduced in Fig. 3, which shows $\overline{n}$ as a function of φ for $\eta=100\%$ and 10%. The uncorrelated value

$$\overline{n}_{\mathrm{uncor}}=2 \tag{3.46}$$

is also indicated in this figure. We observe that the detector clicks are bunched for almost the entire φ range of the plot; antibunching is seen only around $\varphi=\sqrt{2}\,\pi=4.44$. The said value of $\overline{n}_{\mathrm{uncor}}$ results from (3.10) after noting that Eqs. (3.11) yield

$$r_A=\tfrac{1}{2}\eta_A r,\quad r_B=\tfrac{1}{2}\eta_B r \tag{3.47}$$

for the $\mathcal{A}$ and $\mathcal{B}$ operators of (2.13); thus $r_A=r_B$ holds for $\eta_A=\eta_B=\eta$ and (3.46) obtains.

More generally, we have

$$\left.\begin{matrix}\mathrm{tr}\{\mathcal{A}\rho\}\\ \mathrm{tr}\{\mathcal{B}\rho\}\end{matrix}\right\}=\tfrac{1}{2}\,\mathrm{tr}\{\rho\}\mp\tfrac{1}{2}\,\mathrm{tr}\,\{(S_B^\dagger S_A+S_A^\dagger S_B)\rho\}, \tag{3.48}$$

with S_A and S_B given in (2.4). Because of the extra $a^\dagger$ ladder operator in S_B, the second trace vanishes unless the number-

state matrix of ρ has nonzero entries on the $k=\pm 1$ diagonals, that is on the first side diagonals. Therefore, we have the rather explicit statements

$$\mathrm{tr}\{\mathcal{A}\rho_{k,n}^{(\eta)}\}=\begin{cases}\frac{1}{2}\delta_{n,0} & \text{for} \quad k=0\\ -\frac{1}{2}\,\mathrm{tr}\{S_B^\dagger S_A\,\rho_{1,n}^{(\eta)}\} & \text{for} \quad k=1\\ -\frac{1}{2}\,\mathrm{tr}\{S_A^\dagger S_B\,\rho_{-1,n}^{(\eta)}\} & \text{for} \quad k=-1\\ 0 & \text{for} \quad k=\pm\,2,\pm\,3,\ldots\end{cases} \tag{3.49}$$

for the right eigenstates $\rho_{k,n}^{(\eta)}$ of $\mathcal{L}^{(\eta)}$. Upon employing the factorization (3.41), the $k=\pm 1$ cases appear as

$$\begin{aligned}\mathrm{tr}\{\mathcal{A}\rho_{-1,n}^{(\eta)}\}&=(\mathrm{tr}\{\mathcal{A}\rho_{1,n}^{(\eta)}\})^*\\ &=-\tfrac{1}{2}\,\mathrm{tr}\{\sin(\varphi\sqrt{a^\dagger a+1}\,)\\ &\quad\times\cos(\varphi\sqrt{a^\dagger a+2}\,)f_{-1,n}^{(\eta)}(a^\dagger a)\}\equiv-\tfrac{1}{2}\alpha_n^{(\eta)}.\end{aligned} \tag{3.50}$$

For the double sum in (3.45) we need to supplement this with

$$\mathrm{tr}\{\check{\rho}_{0,0}^{(\eta)}\mathcal{B}\rho^{(\mathrm{SS})}\}=\mathrm{tr}\{\mathcal{B}\rho^{(\mathrm{SS})}\}=\tfrac{1}{2} \tag{3.51}$$

and

$$\begin{aligned}\mathrm{tr}\{\check{\rho}_{-1,n}^{(\eta)}\mathcal{B}\rho^{(\mathrm{SS})}\}&=(\mathrm{tr}\{\check{\rho}_{1,n}^{(\eta)}\mathcal{B}\rho^{(\mathrm{SS})}\})^*\\ &=\tfrac{1}{4}\,\mathrm{tr}\{\check{f}_{-1,n}^{(\eta)}(a^\dagger a)\sin(2\varphi\,\sqrt{a^\dagger a+1}\,)\\ &\quad\times\rho^{(\mathrm{SS})}(a^\dagger a)\}\equiv\tfrac{1}{2}\check{\beta}_n^{(\eta)}.\end{aligned} \tag{3.52}$$

In view of (3.49) only the $k=0$, $n=0$ term and the $k=\pm 1$ terms contribute to $\overline{n}$ in (3.45). We recall the value of $\lambda_{0,0}^{(\eta)}$ given in (3.44) and arrive at

$$\overline{n}=\left(\frac{1}{2}-\eta r\,\mathrm{Re}\sum_{n=0}^{\infty}\alpha_n^{(\eta)}\check{\beta}_n^{(\eta)}/\lambda_{-1,n}^{(\eta)}\right)^{-1}. \tag{3.53}$$

Please note that the $k=0$, $n=0$ term alone would yield $\overline{n}=2$, which is the value of $\overline{n}_{\mathrm{uncor}}$ of (3.46), so that the $k=\pm 1$ terms account for the correlation effects.

With the analytical expression (3.53) at hand, we can compute $\overline{n}$ in a tiny fraction of the time needed to perform the corresponding Monte Carlo calculation. We have already mentioned at Eq. (3.29) that the solution of the eigenvalue problem (3.25) consumes most of the time. If one does not care about the eigenvalues, the t integral of (3.21) can be evaluated directly. The computation time is then reduced further, roughly by a factor of 2.

More important, however, than this progress at the numerical front is the analytical information contained in (3.53). We learn which aspects of the OAM dynamics are studied in a measurement of $\overline{n}$. The dynamical sector governed by $\mathcal{L}^{(\eta)}$ is relevant, not the one where $\mathcal{L}^{(0)}$ rules. We shall have more to say about this essential distinction in Sec. IV.

A first application is presented in Fig. 4, which shows $\overline{n}$ as a function of the Rabi angle φ for the same parameters

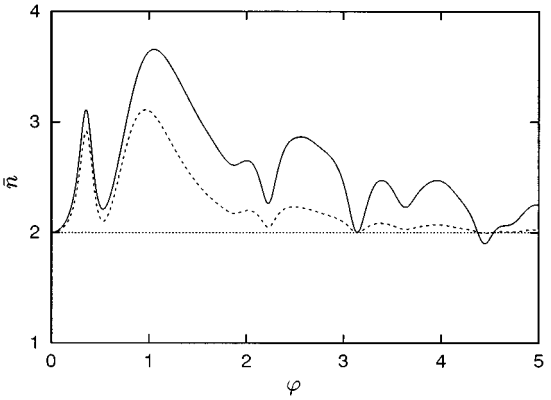

FIG. 4. Analytical results produced by Eq. (3.53) for the same parameter values as in Fig. 3. The two curves are for detector efficiencies of $\eta=100\%$ $(-)$ and $\eta=10\%$ $(---)$; the value of two for uncorrelated detector clicks is indicated as well $(\cdots\cdots)$.

that were used in the Monte Carlo simulation of Fig. 3. The agreement could not be better. In particular, the antibunching around $\varphi=\sqrt{2}\pi=4.44$ is predicted both by the Monte Carlo method and by the analytical formula (3.53).

Whereas this antibunching appears as an exception in Figs. 3 and 4, it is the rule in Fig. 5(a), in which the Rabi angle covers the range $5<\varphi<10$. Thus we observe that the detector clicks tend to be bunched for small Rabi angles and antibunched for larger ones; but, unfortunately, we do not have an intuitive, qualitative understanding of this observation presently.

In Refs. [3–5] a certain similarity was noted, for $\varphi<5$, between the φ dependence of $\overline{n}$ and the mean photon number

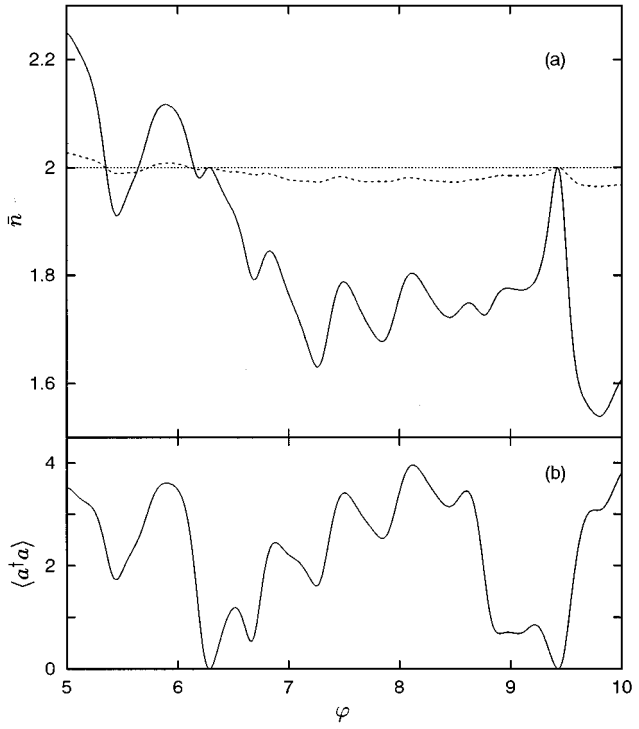

FIG. 5. (a) Same as Fig. 4 for the range $5<\varphi<10$. (b) The corresponding mean number of photons in the cavity field.

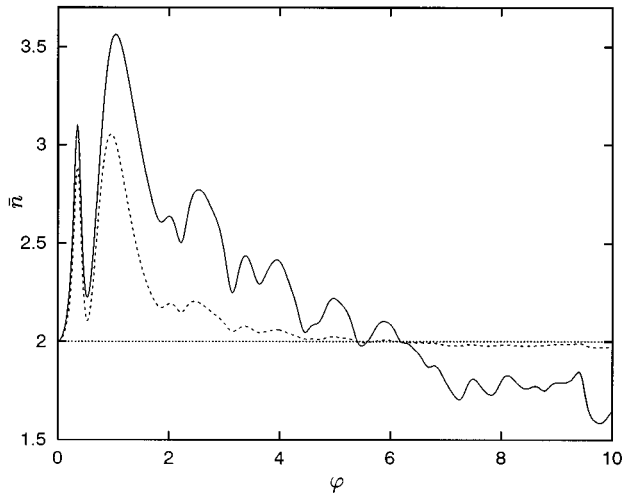

FIG. 6. Mean number $\overline{n}$ of successive detector clicks of the same kind in the phase-sensitive setup of Fig. 1(b) or 1(c) at finite temperature. For $r/\Gamma=25/3$ and $\nu=0.1$, the values of $\overline{n}$ are shown for Rabi angles in the range $0<\varphi<10$ and for detector efficiencies of $\eta=100\%$ $(-)$ and $\eta=10\%$ $(---)$; the value of 2 for uncorrelated detector clicks is indicated as well $(\cdots\cdots)$.

$\langle a^\dagger a\rangle$ in steady state. We believe that this similarity is accidental, because $\overline{n}$ and $\langle a^\dagger a\rangle$ are rather dissimilar functions of φ in the range $5<\varphi<10$, as is clearly visible in Figs. 5(a) and 5(b).

All data presented in Figs. 3–5 refer to the limiting situation of temperature zero. The so-called trapped vacuum states of the OAM are then realized for $\varphi=\pi,2\pi,3\pi,\ldots$. These Rabi angles are such that an excited atom that enters an empty resonator undergoes one, two, three, etc. full Rabi cycles and so leaves the cavity in its excited state. In effect, the atoms are not pumping the resonator at all and the steady state of the cavity field is simply the photon vacuum, irrespective of the beam rate r. Since all emerging atoms are in state $|A\rangle$ before they are exposed to the $\pi/2$ pulse of Fig. 1(b), the detectors will register uncorrelated clicks at the rates (3.47). For symmetric detection these rates are equal and we expect $\overline{n}=\overline{n}_{\rm uncor}=2$ at $\varphi=\pi,2\pi,3\pi,\ldots$. This is confirmed by Figs. 4 and 5(a).

For finite temperatures, there are no trapped vacuum states and the arguments that feed the expectation of $\overline{n}=2$ for $\varphi=\pi,2\pi,3\pi,\ldots$ are no longer valid. Indeed, we find the $\eta=100\%$ values of $\overline{n}=2.248$, 1.993, and 1.835 for $\varphi/\pi=1$, 2, and 3, respectively, when $r/\Gamma=25/3$ and $\nu=0.1$. For this value of the thermal photon number, the φ dependence of $\overline{n}$ is plotted in Fig. 6 whereby all other parameters are the same as in Figs. 4 and 5. Not surprisingly, we observe that the thermal noise leads to a smoothing of the $\overline{n}$-of-φ curve, but the strong tendencies toward bunching for $\varphi\lesssim 6$ and toward antibunching for $\varphi\gtrsim 6$ are equally pronounced for $\nu=0.1$ as they are for $\nu=0$.

5. Standard setup

For the standard OAM setup of Fig. 1(a), the operators $\mathcal{A}$ and $\mathcal{B}$ are given in (2.6) and (2.8) and therefore the *a priori* rates of (3.11) are

$$r_{\rm A}=r\eta_{\rm A}\,{\rm tr}\{\cos^2(\varphi\sqrt{aa^\dagger})\,\rho^{\rm (SS)}(a^\dagger a)\}$$
$$\equiv r\eta_{\rm A}\langle\cos^2(\varphi\sqrt{aa^\dagger})\rangle^{\rm (SS)} \tag{3.54}$$

and

$$r_{\rm B}=r\eta_{\rm B}\,{\rm tr}\{\sin^2(\varphi\sqrt{aa^\dagger})\rho^{\rm (SS)}(a^\dagger a)\}$$
$$=r\eta_{\rm B}\langle\sin^2(\varphi\sqrt{aa^\dagger})\rangle^{\rm (SS)}. \tag{3.55}$$

Since the equality

$$\Gamma(\langle a^\dagger a\rangle^{\rm (SS)}-\nu)=r\langle\sin^2(\varphi\sqrt{aa^\dagger})\rangle^{\rm (SS)} \tag{3.56}$$

holds for the OAM steady state (2.14) — incidentally, this equates the thermal loss rate to the pump gain rate and thus states the energy balance in steady state — we can express $r_{\rm A}$ and $r_{\rm B}$ in terms of the mean photon number $\langle a^\dagger a\rangle^{\rm (SS)}$,

$$r_{\rm A}=\eta_{\rm A}r-\eta_{\rm A}\Gamma(\langle a^\dagger a\rangle^{\rm (SS)}-\nu),$$
$$r_{\rm B}=\eta_{\rm B}\Gamma(\langle a^\dagger a\rangle^{\rm (SS)}-\nu). \tag{3.57}$$

When inserted into (3.10) these *a priori* rates supply us with the value of $\overline{n}_{\rm uncor}$. In particular, we find

$$\overline{n}_{\rm uncor}=\frac{r^2}{2\Gamma^2}[(\langle a^\dagger a\rangle^{\rm (SS)}-\nu)(r/\Gamma-\langle a^\dagger a\rangle^{\rm (SS)}+\nu)]^{-1} \tag{3.58}$$

if the detection is symmetric $\eta_{\rm A}=\eta_{\rm B}=\eta$.

The operators $\mathcal{A}$ and $\mathcal{B}$ of (2.6) and (2.8) do not couple different diagonals of the statistical operator ρ. Accordingly, the eigenstates of $\mathcal{L}^{(\eta)}$ are of the form (3.41) even if the detector efficiencies $\eta_{\rm A}$ and $\eta_{\rm B}$ are not the same. Nevertheless, we shall be content with treating the symmetric detection scheme because then the same eigenvalues and eigenstates can be used as in Sec. III C 4.

As a consequence of the decoupling between the diagonals, now only the $k=0$ terms contribute to the sum in (3.45) because both traces therein vanish for $k\neq 0$. Further, similar to the observation made at Eq. (3.53), the $k=0$, $n=0$ term alone would yield $\overline{n}_{\rm uncor}$ of (3.58) here too; the $k=0$, $n>0$ terms account for the correlation effects. The analog of (3.53) thus reads

$$\overline{n/n}_{\rm uncor}=\left(1+2\eta r\overline{n}_{\rm uncor}\sum_{n=1}^{\infty}\chi_n\check{\psi}_n/\lambda_{0,n}^{(\eta)}\right)^{-1} \tag{3.59}$$

with the symbols χ_n and $\check{\psi}_n$ defined by

$$\chi_n\equiv{\rm tr}\{\mathcal{A}\rho_{0,n}^{(\eta)}\}={\rm tr}\{\cos^2(\varphi\sqrt{aa^\dagger})f_{0,n}^{(\eta)}(a^\dagger a)\},$$
$$\check{\psi}_n\equiv{\rm tr}\{\check{\rho}_{0,n}^{(\eta)}\mathcal{B}\rho^{\rm (SS)}\}=\langle\check{f}_{0,n}^{(\eta)}(aa^\dagger)\sin^2(\varphi\sqrt{aa^\dagger})\rangle^{\rm (SS)}, \tag{3.60}$$

where the $a^\dagger a$ functions introduced in (3.41) appear.

In (3.59) we have normalized $\overline{n}$ to $\overline{n}_{\rm uncor}$ because this ratio tells us whether the clicks are bunched or antibunched. Whereas it is clear that the right-hand side of (3.59) could be evaluated for many different parameter sets, that would be rather pointless. We demonstrate the case with the plots of Fig. 7. They show $\overline{n/n}_{\rm uncor}$ as a function of φ for

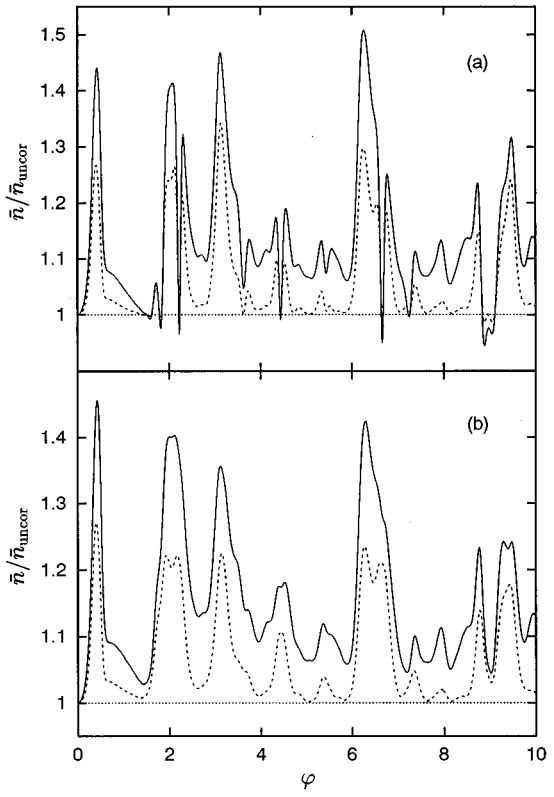

FIG. 7. Mean number of successive detector clicks of the same kind in the standard setup of Fig. 1(a), normalized to the value for uncorrelated clicks. For $r/\Gamma = 25/3$, the ratio $\overline{n/n_{\rm uncor}}$ is shown for Rabi angles in the range $0<\varphi<10$ and for detector efficiencies of $\eta = 100\%$ $(-)$ and $\eta = 10\%$ $(---)$. The number of thermal photons is (a) $\nu = 0$ or (b) $\nu = 0.1$.

$r/\Gamma = 25/3$ at temperature zero and for $\nu = 0.1$. Antibunching is found only for $\nu = 0$ in a few rather narrow φ intervals and even there $\overline{n}$ is just a few percent short of $\overline{n}_{\rm uncor}$. The thermal noise associated with $\nu = 0.1$ is enough to enforce $\overline{n} > \overline{n}_{\rm uncor}$ over the entire φ range considered.

IV. CORRELATION FUNCTIONS

The phase sensitive setup of Fig. 1(b) was introduced in Refs. [3–5] to enable the experimenter to investigate the dynamics of the electric field in the one-atom maser, in particular its decay to the stationary null value. The quantity of primary interest is the (first-order) photon-photon correlation function

$$g^{(\rm ph)}(t) \equiv \frac{\langle a^\dagger(t)a(0)\rangle^{(\rm SS)}}{\langle a^\dagger a\rangle^{(\rm SS)}} = \frac{\mathrm{tr}\,\{a^\dagger \exp\,(\mathcal{L}^{(0)}t)a\rho^{(\rm SS)}\}}{\mathrm{tr}\,\{a^\dagger a\rho^{(\rm SS)}\}}, \tag{4.1}$$

because its Fourier transform supplies us with the spectrum of the cavity field. Direct measurements of the properties of the photon state are not possible in OAM experiments and therefore $g^{(\rm ph)}(t)$ is a theoretical quantity in the first place and so is the OAM spectrum. All modifications of the standard OAM apparatus that aim at studies of the phase dynamics, such as the setup proposed in Ref. [20] or the phase sensitive one of Fig. 1(b), determine correlations between atoms rather than between photons. In this section we discuss some of the relations between atom-atom and photon-photon correlations.

We express the numerator in (4.1) with the aid of the eigenvalues and eigenstates of $\mathcal{L}^{(0)}$ [the latter in the form of (3.41) with $\eta = 0$] and arrive at

$$g^{(\rm ph)}(t) = \sum_{n=0}^{\infty} w_n^{(\rm ph)} \exp(-\lambda_{-1,n}^{(0)} t), \tag{4.2}$$

where the weights $w_n^{(\rm ph)}$ are given by

$$w_n^{(\rm ph)} = \mathrm{tr}\,\{\sqrt{aa^\dagger}\, f_{-1,n}^{(0)}(a^\dagger a)\} \times \frac{\langle \sqrt{a^\dagger a}\check{f}_{-1,n}^{(0)}(a^\dagger a - 1)\rangle^{(\rm SS)}}{\langle a^\dagger a\rangle^{(\rm SS)}}. \tag{4.3}$$

The sum rule

$$\sum_{n=0}^{\infty} w_n^{(\rm ph)} = 1 \tag{4.4}$$

is implied by $g^{(\rm ph)}(t=0) = 1$, which is the conventional normalization. The term ''weight'' for $w_n^{(\rm ph)}$ is suggestive, but might be misleading since these numbers are not guaranteed to be positive or even real. With this proviso we shall continue to speak of weights.

The eigenvalue analysis performed here is essentially identical to that of Ref. [21], although we are employing different notational conventions. Readers interested in the alternative of a Green's-function approach and analytical approximations based on it should consult Ref. [22].

Both the expression for $\overline{n}$ in Eq. (3.53) and that for $g^{(\rm ph)}(t)$ in (4.2) involve eigenvalues to $k = -1$, but $\eta > 0$ is essential in (3.53) whereas the $\eta = 0$ eigenvalues are needed in (4.2). Therefore, measurements of $\overline{n}$ do not yield any information that could be directly related to the OAM spectrum. It is true that some connections exist in the limit $\eta \to 0$, such as

$$\frac{\partial}{\partial t}\overline{n}\Big|_{\eta=0} = 4r\ \mathrm{Re}\sum_{n=0}^{\infty} \alpha_n^{(0)}\check{\beta}_n^{(0)}/\lambda_{-1,n}^{(0)}; \tag{4.5}$$

these are, however, practically useless for two reasons. First, the left-hand side cannot be determined experimentally because of the vanishing signal-to-noise ratio for $\eta \to 0$; second, the eigenvalues $\lambda_{-1,n}^{(0)}$ cannot be extracted from the sum on the right-hand side. We are thus led to this conclusion: Although measurements of $\overline{n}$ and their comparison with the theoretically predicted values constitute a valuable test of OAM theory — be it for the standard setup or the phase sensitive one — information about the OAM spectrum is not gained in such experiments.

Fortunately, such information is contained in other quantities that characterize the statistics of the detector clicks, in particular in the atom-atom (or rather click-click) correlation function. The generic example is $G_{\rm AB}(t)$, which measures the cross correlation for a B click after time t has elapsed since an A click happened. It is given by [12]

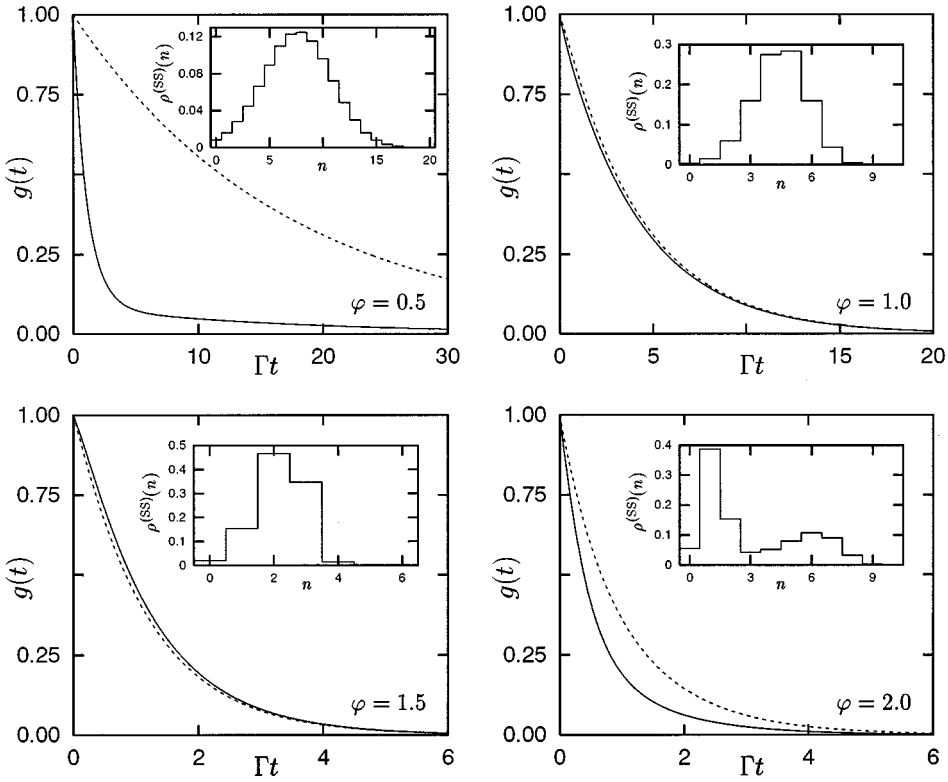

FIG. 8. Reduced atom-atom correlation functions $g^{(\mathrm{at})}(t)$ $(-)$ and photon-photon correlation functions $g^{(\mathrm{ph})}(t)$ $(---)$ for Rabi angles $\varphi=0.5$, 1.0, 1.5, and 2.0. The insets show the corresponding photon probability distributions in steady state. All plots are for $r/\Gamma=25/3$ and $\nu=0$.

$$G_{\mathrm{AB}}(\mathrm{t})=\frac{\mathrm{tr}\,\{\mathcal{B}\exp(\mathcal{L}^{(0)}t)\mathcal{A}\rho^{(\mathrm{SS})}\}}{\mathrm{tr}\,\{\mathcal{B}\rho^{(\mathrm{SS})}\}\,\mathrm{tr}\,\{\mathcal{A}\rho^{(\mathrm{SS})}\}};\tag{4.6}$$

note that there is no dependence on the detector efficiencies. This atom-atom correlation function is normalized according to different conventions than the photon-photon correlation function $g^{(\mathrm{ph})}(t)$ of (4.1). For an easier comparison of the two, we introduce the reduced atom-atom correlation function

$$g^{(\mathrm{at})}(t)=\frac{G_{\mathrm{AB}}(t)-1}{G_{\mathrm{AB}}(0)-1},\tag{4.7}$$

which is subject to the same normalization as $g^{(\mathrm{ph})}(t)$, viz., $g(t=0)=1$ and $g(t=\infty)=0$. This definition of $g^{(\mathrm{at})}(t)$ involves $G_{\mathrm{AB}}(\mathrm{t})$, but for the $\mathcal{A}$ and $\mathcal{B}$ operators of the phase sensitive setup [recall (2.13)] the same $g^{(\mathrm{at})}(t)$ is obtained for $G_{\mathrm{AA}}(t)$, $G_{\mathrm{BB}}(t)$, and $G_{\mathrm{BA}}(t)$. Consequently, $g^{(\mathrm{at})}(t)$ uniquely specifies all the various atom-atom correlation functions in conjunction with their values at $t=0$. In view of $G_{\mathrm{AB}}(0)=G_{\mathrm{BA}}(0)$ and $G_{\mathrm{AA}}(0)=G_{\mathrm{BB}}(0)$, there are really only two of them, not four.

The reduced atom-atom correlation function can be cast into forms that are closely analogous to (4.1) and (4.2),

$$g^{(\mathrm{at})}(t)=\frac{\mathrm{tr}\,\{(\mathcal{B}-\mathcal{A})\exp(\mathcal{L}^{(0)}t)(\mathcal{B}-\mathcal{A})\rho^{(\mathrm{SS})}\}}{\mathrm{tr}\,\{(\mathcal{B}-\mathcal{A})^2\rho^{(\mathrm{SS})}\}}$$

$$=\mathrm{Re}\sum_{n=0}^{\infty}w_n^{(\mathrm{at})}\exp(-\lambda_{-1,n}^{(0)}t),\tag{4.8}$$

where the weights

$$w_n^{(\mathrm{at})}=\frac{\alpha_n^{(0)}\breve{\beta}_n^{(0)}}{\mathrm{Re}\sum_{m=0}^{\infty}\alpha_m^{(0)}\breve{\beta}_m^{(0)}}\tag{4.9}$$

involve the $\eta=0$ versions of the coefficients introduced in Eqs. (3.50) and (3.52). The remark about our sloppy use of the term ''weight,'' made after Eq. (4.4), applies here too. Incidentally, the injunctions to take the real parts of the sums in (4.8) and (4.9) are superfluous because these sums happen to be real themselves, although the individual summands may be complex. The photon-photon correlation function of (4.1) is real as well.

The same eigenvalues that enter the photon-photon correlation function $g^{(\mathrm{ph})}(t)$ of (4.1) determine also the time dependence of $g^{(\mathrm{at})}(t)$. As a rule, the weights $w_n^{(\mathrm{ph})}$ and $w_n^{(\mathrm{at})}$ are different, of course, with the consequence that measurements of $g^{(\mathrm{at})}(t)$ will supply only partial information about $g^{(\mathrm{ph})}(t)$ and therefore about the OAM spectrum.

If the photon-number distribution in steady state is dominated by a single narrow peak, then approximations such as

$$\cos(\varphi\sqrt{aa^\dagger})\rho^{(\mathrm{SS})}(a^\dagger a)\cong\cos(\varphi\sqrt{\langle aa^\dagger\rangle^{(\mathrm{SS})}})\rho^{(\mathrm{SS})}(a^\dagger a),$$

$$\rho^{(\mathrm{SS})}(a^\dagger a)a\cong a\rho^{(\mathrm{SS})}(a^\dagger a)\tag{4.10}$$

are permissible. Accordingly, we have

$$(\mathcal{B}-\mathcal{A})\rho^{(\mathrm{SS})}\cong\frac{\sin(2\varphi\sqrt{\langle aa^\dagger\rangle^{(\mathrm{SS})}})}{2\sqrt{\langle aa^\dagger\rangle^{(\mathrm{SS})}}}(a\rho^{(\mathrm{SS})}+\rho^{(\mathrm{SS})}a^\dagger),\tag{4.11}$$

TABLE I. Those eigenvalues $\lambda^{(0)}_{-1,n}$ of the Liouville operator $\mathcal{L}^{(0)}$, in units of the decay rate Γ, that are most relevant for the correlation functions plotted in Fig. 8, and the weights $w_n^{(\mathrm{ph})}$, $w_n^{(\mathrm{at})}$ associated with them. The eigenvalues are ordered according to the increasing real part; note that some intermediate n values are missing because they carry no weight within the accuracy of the table.

φ	n	$\lambda^{(0)}_{-1,n}/\Gamma$	$w_n^{(\mathrm{ph})}$	$w_n^{(\mathrm{at})}$
0.5	1	0.058	0.998	0.086
	2	0.873	0.003	0.830
	3	1.675	−0.001	0.086
	4	2.650	0.0	−0.002
1.0	1	0.239	1.026	0.979
	2	2.820	−0.026	0.016
	4	4.945	0.0	0.006
	7	6.854	0.0	−0.001
1.5	1	0.762	−0.050	−0.061
	2	0.864	1.084	1.167
	3	2.944	0.002	0.020
	4	$4.279+0.493i$	$-0.013-0.008i$	$-0.056-0.029i$
	5	$4.279-0.493i$	$-0.013+0.008i$	$-0.056+0.029i$
	7	$6.512+0.183i$	$-0.006+0.003i$	$-0.009+0.008i$
	8	$6.512-0.183i$	$-0.006-0.003i$	$-0.009-0.008i$
	11	11.516	0.0	0.004
2.0	1	0.840	0.750	0.305
	2	2.099	0.322	0.298
	4	3.323	−0.075	0.612
	6	$6.035+0.224i$	$0.002+0.003i$	$-0.115-0.001i$
	7	$6.035-0.224i$	$0.002-0.003i$	$-0.115+0.001i$
	9	$8.889+0.208i$	0.0	$0.009-0.012i$
	10	$8.889-0.208i$	0.0	$0.009+0.012i$
	11	9.830	0.0	−0.002

under these circumstances. As pointed out in Ref. [23], there should then not be a significant difference between $g^{(\mathrm{ph})}(t)$ and $g^{(\mathrm{at})}(t)$ and the experimental determination of the latter can be regarded as a measurement of the former.

This observation is confirmed by the plots shown in Fig. 8 (similar plots comparing second-order correlation functions are contained in Ref. [24]). For $\varphi=1$ and $\varphi=1.5$, the requirement of a single narrow peak is met and the two correlation functions are hardly distinguishable. By contrast, $g^{(\mathrm{ph})}(t)$ and $g^{(\mathrm{at})}(t)$ are visibly at variance with each other for $\varphi=0.5$ (one broad peak) and $\varphi=2$ (two peaks). These differences are also exhibited in Table I, where we report the relevant eigenvalues and weights that enter Eqs. (4.2) and (4.8). For $\varphi=1$ and $\varphi=1.5$, we see that a single eigenvalue dominates: the smallest one or the second smallest one, respectively. Single eigenvalues carry also most of the weight for $\varphi=0.5$, but not the same ones for $g^{(\mathrm{ph})}$ and $g^{(\mathrm{at})}$; the latter has substantial contributions from two more eigenvalues. Yet another situation is encountered for $\varphi=2$, where two eigenvalues contribute the largest portion to the photon-photon correlation function, whereas three real eigenvalues and a pair of complex conjugate ones are most relevant for the atom-atom correlations.

We note in passing that the smallest eigenvalue carries negative weight for $\varphi=1.5$. Therefore, the correlation functions are negative for times t sufficiently late. The sign change occurs around $t\cong 30/\Gamma=250/r$, that is after about 30 photon lifetimes during which period an average number of 250 atoms traverse the resonator. Consequently, these (very weak) long-time anticorrelations are of no experimental significance.

In summary, we conclude that a measurement of $g^{(\mathrm{at})}(t)$ will yield those eigenvalues of $\mathcal{L}^{(0)}$ that are most important for the photon-photon correlation function and thus for the OAM spectrum. The weights $w_n^{(\mathrm{ph})}$, however, are not made available in this way, so that the spectrum cannot be inferred. Nevertheless, the comparison of the experimental atom-atom correlation function with the theoretical prediction would once more put OAM theory to the test.

V. SUMMARY

We have reconsidered the phase-sensitive OAM setup proposed in Refs. [3–5] in which the state reduction that is associated with each registered detector click effects a post-selection of the phase of the maser field. In these papers it was surmised that the mean number of successive detector clicks of the same kind supplies information about the phase dynamics of the pumped maser and so tells the experimenter something about the maser spectrum. In the present paper we

derive an analytical expression for this mean number and find perfect agreement with the results obtained in Refs. [3–5] with the aid of a numerical simulation of the OAM dynamics. Unfortunately, the structure of the analytical answer contradicts the said surmise because it involves the eigenvalues of a Liouville operator different from the one that determines the OAM spectrum. As we demonstrate then, the relevant eigenvalues are, however, available from measurements of the atom-atom correlation function, as has been already noted qualitatively in [5] and discussed in more detail in [23]. Partial knowledge about the OAM spectrum can thus be extracted from the statistics of the emerging atoms.

VI. OUTLOOK

Let us close with an outlook on likely future developments. Prior to the interaction with the cavity field there are no correlations among the atoms in the Poissonian beam. The observation of correlations after the interaction therefore indicates that the atoms have become entangled. The primary entanglement is between the photons and the atoms and the atom-atom entanglement is of secondary nature. This secondary entanglement is the origin of the correlations among the detector clicks.

Inasmuch as all such entanglements give rise to correlations of the Einstein-Podolsky-Rosen type [25], one is invited to ask [5] if violations of the Bell inequality [6] can be demonstrated in OAM experiments. By changing the relative phase of the classical field that produces the $\pi/2$ pulse in Fig. 1(b) one could probe the atoms for the various superpositions of $|\mathrm{A}\rangle$ and $|\mathrm{B}\rangle$ that enter the Bell inequality. According to Ref. [26], such violations can be found indeed if one uses a pair of test atoms in addition to the pump atoms of the Poissonian beam. At present it is an open question whether the two-particle correlations among the emerging pump atoms themselves are strong enough. There is also the practical aspect that the detector efficiencies are most likely too small for tests of the Bell inequality.

The detector efficiencies play no role when one looks for correlations of the Greenberger-Horne-Zeilinger (GHZ) type [7,27], which would involve three or more atoms and are much stronger than the two-atom correlations of the Bell inequality. In particular, Mermin's version [28] for three spin-$\frac{1}{2}$ particles is suited perfectly for the two-level atoms used in OAM experiments. A method for preparing a Mermin-type GHZ state was proposed in Ref. [29]. It utilizes the interaction of atoms with photons in a resonator in a clever way. Here too we do not know presently if the three-particle correlations that are built up among the pump atoms as a result of the standard OAM operation are strong enough to allow for experimental studies of GHZ correlations. Investigations along these lines are the intended subject of a future investigation.

ACKNOWLEDGMENT

One of us (Ts.G.) would like to express his gratitude for the financial support by the Alexander von Humboldt-Stiftung.

APPENDIX

Here we demonstrate that $\overline{n}$ of (3.24) reduces to $\overline{n}_{\mathrm{uncor}}$ of (3.10) in the situation of very low detector efficiencies, $0<\eta_{\mathrm{A}},\eta_{\mathrm{B}}\ll 1$. We regard $\eta_{\mathrm{A}},\eta_{\mathrm{B}}$ as infinitesimal quantities and proceed from noting that, under these circumstances, $\mathcal{L}^{(\eta)}$ of (2.17) differs from $\mathcal{L}^{(0)}$ only by an infinitesimal amount. Therefore, the eigenvalues $\lambda_\mu^{(\eta)}$ of $-\mathcal{L}^{(\eta)}$ agree with the eigenvalues $\lambda_\mu^{(0)}$ of $-\mathcal{L}^{(0)}$ up to terms that are linear in $\eta_{\mathrm{A}},\eta_{\mathrm{B}}$:

$$\begin{aligned}\lambda_\mu^{(\eta)}&=\lambda_\mu^{(0)}+\mathrm{tr}\{\check{\rho}_\mu^{(0)}(\mathcal{L}^{(0)}-\mathcal{L}^{(\eta)})\rho_\mu^{(0)}\}\\&=\lambda_\mu^{(0)}+r\,\mathrm{tr}\{\check{\rho}_\mu^{(0)}(\eta_{\mathrm{A}}\mathcal{A}+\eta_{\mathrm{B}}\mathcal{B})\rho_\mu^{(0)}\}.\end{aligned}\tag{A1}$$

In this result of first-order perturbation theory, all contributions of second and higher order in $\eta_{\mathrm{A}},\eta_{\mathrm{B}}$ are consistently disregarded. (The implicit assumption that the eigenvalues are not degenerate is innocuous.)

Now we recall that the OAM steady state $\rho^{(\mathrm{SS})}$ is the (unique) eigenstate of $\mathcal{L}^{(0)}$ to the eigenvalue $\lambda^{(0)}=0$. We associate the label $\mu=0$ with this eigenvalue, so that

$$\lambda_0^{(0)}=0\,,\quad \rho_0^{(0)}=\rho^{(\mathrm{SS})},\quad \check{\rho}_0^{(0)}=1\tag{A2}$$

by convention. Then we have, for $\mu=0$,

$$\lambda_0^{(\eta)}=r\,\mathrm{tr}\{(\eta_{\mathrm{A}}\mathcal{A}+\eta_{\mathrm{B}}\mathcal{B})\rho^{(\mathrm{SS})}\}=r_{\mathrm{A}}+r_{\mathrm{B}},$$

and for $\mu\neq 0$,

$$\lambda_\mu^{(\eta)}=\lambda_\mu^{(0)}\neq 0\tag{A3}$$

for $0<\eta_{\mathrm{A}},\eta_{\mathrm{B}}\ll 1$. Consequently, in the sum over μ that appears in (3.29),

$$\sum_\mu\ \mathrm{tr}\{\eta_{\mathrm{A}}\mathcal{A}\rho_\mu^{(\eta)}\}\frac{r}{\lambda_\mu^{(\eta)}}\,\mathrm{tr}\{\check{\rho}_\mu^{(\eta)}\eta_{\mathrm{B}}\mathcal{B}\rho^{(\mathrm{SS})}\},\tag{A4}$$

the $\mu=0$ term is of first order in $\eta_{\mathrm{A}},\eta_{\mathrm{B}}$ and the $\mu\neq 0$ terms are of second order. The $\mu\neq 0$ terms are therefore negligibly small; with $\rho_0^{(\eta)}\to\rho_0^{(0)}=\rho^{(\mathrm{SS})}$ and $\check{\rho}_0^{(\eta)}\to\check{\rho}_0^{(0)}=1$ the $\mu=0$ term equals

$$\mathrm{tr}\{\eta_{\mathrm{A}}\mathcal{A}\rho^{(\mathrm{SS})}\}\frac{r}{\lambda_0^{(\eta)}}\,\mathrm{tr}\{\eta_{\mathrm{B}}\mathcal{B}\rho^{(\mathrm{SS})}\}=\frac{r_{\mathrm{A}}r_{\mathrm{B}}/r}{r_{\mathrm{A}}+r_{\mathrm{B}}}.\tag{A5}$$

Accordingly, Eq. (3.29) turns into

$$\overline{n}=\frac{r_{\mathrm{A}}+r_{\mathrm{B}}}{2r}\left(\frac{r_{\mathrm{A}}r_{\mathrm{B}}/r}{r_{\mathrm{A}}+r_{\mathrm{B}}}\right)^{-1}=\frac{(r_{\mathrm{A}}+r_{\mathrm{B}})^2}{2r_{\mathrm{A}}r_{\mathrm{B}}}=\overline{n}_{\mathrm{uncor}}.\tag{A6}$$

Since (3.29) is equivalent to (3.24) this completes the demonstration that $\overline{n}$ reduces to $\overline{n}_{\mathrm{uncor}}$ for $0<\eta_{\mathrm{A}},\eta_{\mathrm{B}}\ll 1$.

[1] A recent review of the one-atom maser is given by G. Raithel, C. Wagner, H. Walther, L. M. Narducci, and M. O. Scully, in *Cavity Quantum Electrodynamics*, edited by P. R. Berman (Academic, Boston, 1994), p. 57.

[2] A recent tutorial review of OAM theory is given by B.-G. Englert, in *Physics and Contemporary Needs*, Proceedings of the 19th International Nathiagali Summer College on Physics and Contemporary Needs, Nathiagali, 1994, edited by S. A. Ahmad and S. M. Farooqi (Pak, Islamabad, in press), Vol. 19.

[3] C. Wagner, R. J. Brecha, A. Schenzle, and H. Walther, Phys. Bl. **48**, 465 (1992).

[4] C. Wagner, R. J. Brecha, A. Schenzle, and H. Walther, Phys. Rev. A **46**, R5350 (1992).

[5] C. Wagner, R. J. Brecha, A. Schenzle, and H. Walther, Phys. Rev. A **47**, 5068 (1993).

[6] J. S. Bell, Physics **1**, 195 (1964).

[7] D. M. Greenberger, M. Horne, and A. Zeilinger, in *Bell's Theorem, Quantum Theory, and Conceptions of the Universe*, edited by M. Kafatos (Kluwer, Dordrecht, 1989), p. 107.

[8] There is actually room for additional phase factors, so that the $\pi/2$ pulse could produce equally well the superpositions $(|\mathrm{A}\rangle+i|\mathrm{B}\rangle)/\sqrt{2}$ and $(|\mathrm{B}\rangle+i|\mathrm{A}\rangle)/\sqrt{2}$, for instance. Such phase factors are, however, quite irrelevant. Therefore we simplify matters by absorbing them into the definitions of $|\mathrm{A}\rangle$ and $|\mathrm{B}\rangle$.

[9] P. Filipowicz, J. Javanainen, and P. Meystre, Phys. Rev. A **34**, 3077 (1986).

[10] L. A. Lugiato, M. O. Scully, and H. Walther, Phys. Rev. A **36**, 740 (1987).

[11] L. Davidovich, J. M. Raimond, M. Brune, and S. Haroche, Phys. Rev. A **36**, 3771 (1987).

[12] H.-J. Briegel, B.-G. Englert, N. Sterpi, and H. Walther, Phys. Rev. A **49**, 2962 (1994).

[13] The concept of deliberate ignorance is thoroughly discussed in Ref. [12].

[14] The number $\overline{n}$ is denoted by $\langle N_s\rangle$ in Refs. [3–5].

[15] C. Wagner, A. Schenzle, and H. Walther, Opt. Commun. **107**, 318 (1994).

[16] U. Herzog, Phys. Rev. A **50**, 783 (1994).

[17] Of course, one can find analogous expressions for all probabilities p_n. Without bothering with the details of the derivation, we report the generating function

$$\sum_{n=0}^{\infty} p_n x^n = \frac{r^2}{r_\mathrm{A}+r_\mathrm{B}}\left(\eta_\mathrm{A}^2\,\mathrm{tr}\,\{\mathcal{A}[-\mathcal{L}^{(\eta)}-xr\,\eta_\mathrm{B}\mathcal{B}]^{-1}\mathcal{A}\rho^{(\mathrm{SS})}\}\right.$$
$$\left.+\,\eta_\mathrm{B}^2\,\mathrm{tr}\,\{\mathcal{B}[-\mathcal{L}^{(\eta)}-xr\,\eta_\mathrm{A}\mathcal{A}]^{-1}\mathcal{B}\rho^{(\mathrm{SS})}\}\right).$$

Equation (3.21) is the $x=0$ case thereof and the normalization (3.2) is stated for $x=1$. The latter assertion can be checked with the technical means used in establishing the identities (3.22). The verification of the statement (3.3) needs the operator identity

$$\frac{\partial}{\partial x}\frac{1}{\mathcal{F}(x)} = -\frac{1}{\mathcal{F}(x)}\frac{\partial \mathcal{F}(x)}{\partial x}\frac{1}{\mathcal{F}(x)}$$

in addition.

[18] H.-J. Briegel and B.-G. Englert, Phys. Rev. A **47**, 3311 (1993).

[19] M. Elk and B.-G. Englert (unpublished).

[20] M. O. Scully, H. Walther, G. S. Agarwal, T. Quang, and W. Schleich, Phys. Rev. A **44**, 5992 (1991).

[21] K. Vogel, W. P. Schleich, M. O. Scully, and H. Walther, Phys. Rev. A **48**, 813 (1993).

[22] T. Quang, G. S. Agarwal, J. Bergou, M. O. Scully, H. Walther, K. Vogel, and W. P. Schleich, Phys. Rev. A **48**, 803 (1993).

[23] C. Wagner, Doctoral thesis, University of Munich, 1994 (unpublished).

[24] J. D. Cresser and S. M. Pickles, Phys. Rev. A **50**, R925 (1994).

[25] A. Einstein, B. Podolsky, and N. Rosen, Phys. Rev. **47**, 777 (1935).

[26] P. Masiak and K. Rzążewski, Appl. Phys. B **60**, S17 (1995); **61**, 125 (E) (1995).

[27] D. M. Greenberger, M. Horne, A. Shimony, and A. Zeilinger, Am. J. Phys. **58**, 1131 (1990).

[28] N. D. Mermin, Am. J. Phys. **58**, 731 (1990); Phys. Today **43** (6), 9 (1990).

[29] K. Wódkiewicz, L. Wang, and J. H. Eberly, Phys. Rev. A **47**, 3280 (1993).